Analysis of Solar-Heated Thermal Wadis to Support Extended-Duration Lunar Exploration

R. Balasubramaniam,[*] S. Gokoglu,[†] and K. Sacksteder[‡]
NASA John H. Glenn Research Center at Lewis Field, Cleveland, Ohio 44135
R. Wegeng[§]
Pacific Northwest National Laboratory, Richland, Washington 99352
and
N. Suzuki[¶]
NASA Headquarters, Washington, District of Columbia 20546

The realization of the renewed exploration of the moon presents many technical challenges; among them is the survival of lunar-surface assets during periods of darkness when the lunar environment is very cold. Thermal wadis are engineered sources of stored solar energy using modified lunar regolith as a thermal storage mass that can supply energy to protect lightweight robotic rovers or other assets during the lunar night. This paper describes an analysis of the performance of thermal wadis based on the known solar illumination of the moon and estimates of producible thermal properties of modified lunar regolith. Analysis has been performed for the lunar equatorial region and for a potential outpost location near the lunar south pole. The calculations indicate that thermal wadis can provide the desired thermal energy and temperature control for the survival of rovers or other equipment during periods of darkness.

Nomenclature

C_p, C_p'	=	specific heat of the wadi and regolith, respectively, J/(kg · K)
d	=	depth of the wadi, m
$d' - d$	=	depth of the regolith layer underlying the wadi, m
f, f_j	=	periodic surface heat flux in the medium as a function of time and in a time interval j, W/m^2
k, k'	=	thermal conductivity of the wadi and regolith, respectively, W/(m · K)
N, N'	=	scaled depth of the wadi ($d/\sqrt{\alpha t_0}$) and the regolith layer [$(d' - d)/\sqrt{\alpha' t_0}$], respectively
q	=	solar flux impinging on the wadi surface, W/m^2
$\bar{q}$	=	q/q_{max}, scaled solar flux
q_{max}	=	peak solar flux, W/m^2
q_{rov}	=	heat flux supplied to the rover, W/m^2
$\bar{q}_{rov}$	=	$q_{rov}/(\alpha_{abs} q_{max})$, scaled rover heat flux
T, T'	=	temperature distribution as a function of x and t in the wadi and the underlying regolith layer, K
T_a	=	environment temperature, K
$\bar{T}_a$	=	T_a/T_{ref}, scaled environment temperature
T_i	=	initial temperature of the wadi, K
T_{ref}	=	reference temperature, $(\alpha_{abs} q_{max}/\epsilon_0 \sigma)^{1/4}$, K
T_s	=	surface temperature of the wadi, K
t	=	time, s
t_0	=	one half of the synodic period on the moon (354 h), s
x	=	coordinate in the vertical direction into the wadi and the underlying regolith, m
α, α'	=	thermal diffusivities of the wadi and regolith, respectively, m^2/s
α_{abs}	=	radiative absorptivity of the wadi surface
β	=	dimensionless parameter, $(1/\sqrt{2})(k'/k)\sqrt{\alpha/\alpha'}$
ϵ	=	radiative emissivity of the wadi surface
$\bar{\epsilon}$	=	ϵ/ϵ_0, scaled emissivity of the wadi surface
ϵ_0, ϵ_1	=	daytime and nighttime emissivity, respectively, of the wadi surface
θ, θ'	=	scaled temperature distribution in the wadi (T/T_{ref}) and the underlying regolith layer (T'/T_{ref})
λ	=	dimensionless parameter, $k/[\sqrt{\alpha t_0}(\epsilon_0\sigma)^{1/4}(\alpha_{abs} q_{max})^{3/4}]$
ξ	=	scaled coordinate in the vertical direction, $(d - x)/d$ for $0 \le x \le d$ and $(x - d)/(d' - d)$ for $d \le x \le d'$
ρ, ρ'	=	densities of the wadi and regolith, respectively, kg/m^3
σ	=	Stefan–Boltzmann constant, 5.67×10^{-8} W/(m^2 · K^4)
τ	=	scaled time, t/t_0
ϕ_j	=	periodic scaled surface heat flux in the medium in the time interval j in Jaeger's method

I. Introduction

NASA plans to establish a permanent, manned outpost on the moon, and many systems are under development as part of NASA's plans to deploy in situ resource utilization capabilities at the lunar outpost. There is a need to protect the exploration systems from the extreme cold of the lunar surface. Large temperature swings are experienced at most locations on the moon, in part because of its slow rotation rate (the diurnal cycle of the moon is about 29 Earth-days long) and in part because native lunar regolith is very resistant to thermal conduction. Heat does not penetrate very deeply: the characteristic penetration depth is approximately 10 cm during periods of sunlight and, as a result, temperatures typically range from a high of about 400 K to a low of about 100 K. At the present time, for
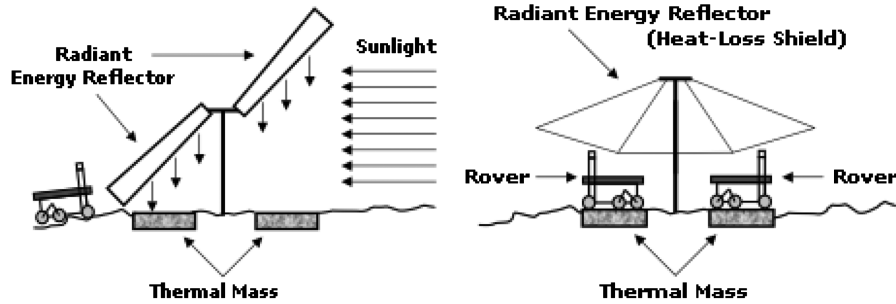
Fig. 1   The lunar thermal wadi concept. On the left, a sun-tracking reflector directs sunlight onto a thermal mass during periods of solar illumination while rovers conduct lunar-surface operations. On the right, rovers are thermally coupled to the thermal mass to stay warm during periods of darkness and are further protected by a heat-loss shield to limit radiative losses to space.

planning purposes, the outpost is assumed to be located in very close proximity to the south pole of the moon, on the rim of Shackleton crater. This location is valued largely because it experiences nearly constant sunlight.** Although the sun must always be at or near the horizon in this location, the small tilt of the moon's axis with respect to the ecliptic results in short periods of darkness, primarily when nearby topographic features cast shadows on this location. Presently, the longest period of darkness is estimated to be 52 h.

In this paper, we present the model formulation, details of the thermal analysis, and results of an effort to examine one aspect of the technical feasibility of using thermal wadis (engineered sources of heat and power [1,2]) that can protect exploration systems from the extreme cold of the lunar surface. The idea is that moderate temperature cycles would be obtained with materials that have a higher thermal conductivity than the native regolith. Accordingly, it has been hypothesized that materials with acceptable properties for thermal energy storage can be produced by using solar energy to sinter and/or melt lunar regolith, allowing it to coalesce into a continuous mass. Indeed, the use of molten regolith as a means of thermal energy storage on the moon was considered for a solar-dynamic power system [3]. Along with additional hardware to regulate the absorption and loss of thermal energy, the resulting thermal mass would experience a reduced temperature swing and could serve as a warming pad for robotic rovers or other exploration assets during periods of darkness on the lunar surface.

The basic concept of a thermal wadi is illustrated in Fig. 1 and consists of a thermal mass plus one or more energy reflectors for a) reflecting solar energy onto the thermal mass during periods of sunlight and b) reflecting radiant energy back to the thermal mass during periods of darkness. During periods of sunlight, thermal energy is absorbed and stored within the thermal mass. During periods of darkness, the stored energy is used to provide temperature control for rovers and other exploration assets. The thermal property values of the thermal mass are critical to the effectiveness of the thermal wadi. In its native state, lunar regolith is a poor material for thermal energy storage. Because of its very low thermal diffusivity, about 6.6×10^{-9} m²/s per measurements made during the Apollo program [4], heat does not penetrate the lunar surface very deeply and is lost rapidly due to radiation during periods of darkness. We show later that the large surface-temperature swing during the moon's 27-day diurnal cycle is controlled by the value of $k'/\sqrt{\alpha'}$ (may also be written as $\sqrt{k'\rho'C_p'}$), which is approximately 123 W$\sqrt{s}/(m^2 \cdot K)$ for native regolith. The regolith, however, contains the elemental materials from which a reasonable thermal energy storage medium can be fabricated, and experiments on Earth have demonstrated that solar and/or microwave energy can enable the necessary conversion processes. Examples of regolith processing methods that can produce thermal masses with improved thermal properties include compacting and sintering [5], melting and solidification of processed or unprocessed regolith, inclusion of materials with high-thermal conductivity and/or high-thermal capacity, and chemically reducing regolith by thermochemical or electrochemical means [6] to produce

a metal-enriched product. Several technical issues must be resolved in order to show that thermal wadis can be a valuable adjunct element of the lunar-surface architecture, including whether thermal-mass material can be readily produced at a reasonable cost on the lunar surface.

Our objective in this paper is to analyze the extent to which a thermal wadi can provide temperature control for a robotic rover based on several simplified configurations of operational hardware and modifications to the native regolith for creating the wadi thermal mass. We present the model formulation and results of a thermal analysis of various wadi concepts to determine the temperature of the thermal mass. As the wadi surface is the simplest interface to any hardware the wadi would support during periods of lunar darkness, the surface temperature is especially of interest. The analysis was performed for simulated conditions at two locations: 1) near the lunar equator, where the solar illumination of the surface can be considered periodic and similar over wide areas, and 2) a single selected site near the lunar south pole, where the illumination is quite irregular but considered a promising site for the planned lunar outpost.

II.   Model

The objective of the thermal analysis is to determine the temperature of the wadi, especially how the wadi-surface temperature varies with time, how the maximum and minimum surface temperatures depend on the incident solar flux, the depth of the wadi, its thermal properties (such as its thermal conductivity, diffusivity, and radiative properties), and coverage of the wadi surface by a thin layer of dust. Also of interest are the contributions of operational hardware that might accompany the thermal wadi, including a reflector of solar illumination that tracks the movement of the sun with respect to the wadi surface and a reflector that limits the radiative loss from the surface of the thermal mass to space, as well as a typical rover that may need to be heated overnight. Throughout our analysis, we use the thermal properties, summarized in Table 1, of native regolith and basalt rock. The latter is the parent material from which regolith is formed. As mentioned before, various processing methods can be used to improve the thermal properties of the regolith close to those of solid basalt.

We assume that the solar flux incident on the surface is spatially uniform and varies with time (e.g., Fig. 2 for the equatorial region). The depth of the wadi is likely to be shallow compared with its lateral extent, so that the wadi can be easily constructed. The thermal conductivity of the wadi material is expected to be much larger than that of native regolith. Within the bulk of the wadi, we therefore expect negligible lateral heat loss to the surrounding regolith, and heat will be transferred primarily in the downward direction. A one-dimensional analysis is therefore sufficient to discern the thermal behavior of the wadi. A one-dimensional analysis has an added benefit of being relatively simple compared with a multidimensional analysis, and it is sufficient to determine the sensitivity of various design options and system parameters on the maximum and minimum surface temperatures of the wadi.

Our thermal model of the wadi is similar to the Wesselink model of thermal energy transfer in planetary regolith [7]. In this model, the

**Data available at http://www.nasa.gov/pdf/163896main_LAT_GES_1204.pdf [retrieved 23 September 2010].

Table 1 Physical properties of wadi materials

Properties	Native regolith	Basalt rock
Thermal diffusivity	6.6×10^{-9} m^2/s	8.7×10^{-7} m^2/s
Density	1800 kg/m^3	3000 kg/m^3
Specific heat	840 J/(kg · K)	800 J/(kg · K)
Thermal conductivity	0.01 W/(m · K)	2.1 W/(m · K)

solar flux that impinges on the material is either absorbed or reflected by its surface. Thermal energy transport beneath the surface is solely by conduction, and there is no radiative flux within the material. Radiative heat loss is allowed only from the surface into space. Jaeger [8] has used such a model to predict the periodic steady-state temperature of the surface of the moon. In Jaeger's model, the incident solar flux has a sinusoidal dependence with time during the lunar day and a vanishing flux during the lunar night. The physical properties of the regolith layer (treated to be infinitely deep) and the radiative properties of its surface are assumed constant with respect to both space and time. Both Wesselink [7] and Jaeger [8] assumed that the emissivity of the lunar surface was unity in their models. The reflectance of lunar mare basalt samples and lunar regolith samples from various locations has been measured in the visible and near-infrared spectrum [4] and is generally in the range of 0.05 to 0.3. In our model, we will assume that the absorptivity of the wadi surface is constant and equal to 0.9 over the wavelength spectrum of the incident solar radiation. The native emissivity of the wadi surface is also assumed to be a constant and equal to 0.9 in the wavelength spectrum of the emitted radiation (infrared region). Our values for the absorptivity and emissivity are consistent with those used in thermal models in the literature for the surface of Mercury (Mitchell and de Pater [9], who used 0.88 and 0.9 for the absorptivity and emissivity, respectively) and the surface of Mercury and the moon (Vasavada et al. [10], who used 0.9 and 0.95 for the absorptivity and emissivity, respectively). Mitchell and de Pater [9] point out that the precise values of the absorptivity and emissivity are not critical, since the surface temperature depends on the fourth root of these quantities. In most of the cases that we model, we assume that a radiation shield is used during the night to reduce the radiative loss from the wadi surface. In such cases, we assume that the effect of the radiation shield can be represented by reducing the surface emissivity of the wadi to an effective value. If the wadi surface and the radiation shield are flat with dimensions that are large relative to their separation distance and are isothermal (but at unequal temperatures), and the environment to which the shield is exposed is regarded as a black-body, it can be shown from energy considerations that the effect of the radiation shield is accommodated by an effective emissivity of the wadi surface that is given by $\epsilon_{eff} = 1/(1/\epsilon_{wadi} + 2/\epsilon_{shield} - 1)$. If the wadi surface behaves close to a blackbody (we assume $\epsilon_{wadi} = 0.9$ in this study) and the shield has an emissivity of about 0.5, then the effective wadi-surface emissivity is about 0.25. Smaller emissivity values of the wadi surface or the shield result in smaller effective wadi-surface emissivities. We choose to use a relatively conservative effective wadi-surface emissivity of 0.25 in this study. In most of the calculations, we assume that energy is supplied from the surface of the wadi to a rover to keep it warm during the lunar night. We represent the energy transfer from the wadi to the rover by a constant
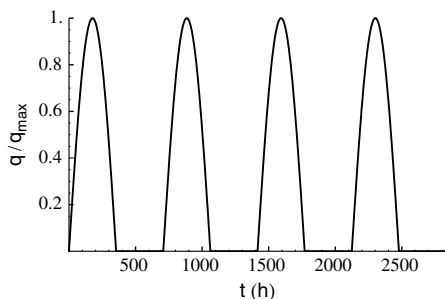
Fig. 2 Equatorial solar flux. The solar flux profile is a semisinusoid.

nighttime surface heat flux (a typical value is 25 W/m^2, as shown later). In reality, the temperature of the rover is expected to be time dependent as it loses heat to the surroundings; therefore, the rate of energy transfer between the wadi and the rover would be time dependent as well. No attempt is made in this study to model the thermal response of the rover.

Within the bulk of the wadi, there is a balance between energy storage (due to sensible heat) and energy transfer by conduction. The bottom boundary of the wadi is assumed to be in contact with native regolith. At this interface, the temperature and heat flux are assumed to be continuous. To model the unbounded extent of regolith that exists beneath the wadi, a finite regolith layer of suitable thickness must be chosen in the numerical calculations. In most of the calculations that we report, the native regolith-layer thickness beneath the wadi was assumed to be 20 cm, which is shown to be adequate later. The characteristic thermal penetration depth in native regolith is $\sqrt{\alpha' t_0}$, where t_0 is one half of the synodic period on the moon ($t_0 \approx 354$ h) and is approximately 9 cm. The bottom boundary of the layer of native regolith is considered to be adiabatic.

Based on the previous model, the equations governing the transfer of energy in the wadi and the underlying regolith, respectively, are

$$\frac{\partial T}{\partial t} = \alpha \frac{\partial^2 T}{\partial x^2} \quad 0 \leq x \leq d \qquad (1)$$

$$\frac{\partial T'}{\partial t} = \alpha' \frac{\partial^2 T'}{\partial x^2} \quad d \leq x \leq d' \qquad (2)$$

The boundary conditions are

$$-k\frac{\partial T}{\partial x} = \alpha_{abs}q(t) - \sigma\epsilon(t)(T^4 - T_a^4) - q_{rov}(t) \quad \text{at } x = 0 \qquad (3)$$

$$T = T', \qquad k\frac{\partial T}{\partial x} = k'\frac{\partial T'}{\partial x} \quad \text{at } x = d \qquad (4)$$

$$\frac{\partial T'}{\partial x} = 0 \quad \text{at } x = d' \qquad (5)$$

The emissivity of the wadi surface is ϵ_0 (typically 0.9) during the day when the incident solar flux is nonzero, and it is ϵ_1 (typically 0.25) during the nighttime when a heat-loss-limiting radiation shield is used. Similarly, q_{rov} is zero during the day and is a specified constant (typically 25 W/m^2) during the night. As an initial condition, we assume that $T = T' = T_i$, where T_i is a constant, typically taken to be 100 K. T_a is the sky or environment temperature for radiative heat loss, and it is set to zero in the calculations. The equations and boundary conditions were solved numerically, as an initial value problem, using the software Mathematica, which uses the method of lines for the solution of partial differential equations.

A. Dimensionless Formulation of the Governing Equations

To determine the dimensionless parameters that control the behavior of the system of equations and boundary conditions given previously, we cast the system in terms of the following dimensionless variables:

$$\theta = \frac{T}{T_{ref}}; \qquad \theta' = \frac{T'}{T_{ref}}; \qquad \tau = \frac{t}{t_0}$$

$$\xi = \frac{d-x}{d} \quad \text{for } 0 \leq x \leq d, \qquad \xi = \frac{x-d}{d'-d} \quad \text{for } d \leq x \leq d'$$

$$\bar{q} = \frac{q}{q_{max}}; \qquad \bar{\epsilon} = \frac{\epsilon}{\epsilon_0}; \qquad \bar{q}_{rov} = \frac{q_{rov}}{\alpha_{abs}q_{max}}$$

$$T_{ref} = \left(\frac{\alpha_{abs}q_{max}}{\epsilon_0\sigma}\right)^{1/4}$$

$$\frac{\partial\theta}{\partial\tau} = \frac{1}{N^2}\frac{\partial^2\theta}{\partial\xi^2} \qquad (6)$$

$$\frac{\partial \theta'}{\partial \tau} = \frac{1}{N'^2} \frac{\partial^2 \theta'}{\partial \xi^2} \tag{7}$$

$$\frac{\lambda}{N} \frac{\partial \theta}{\partial \xi} = \bar{q}(\tau) - \bar{\epsilon}(\tau)(1 - \bar{T}_a^4) - \bar{q}_{\mathrm{rov}}(\tau); \qquad \frac{\partial \theta'}{\partial \xi} = 0 \quad \text{at } \xi = 1 \tag{8}$$

$$\theta = \theta', \qquad \frac{\partial \theta}{\partial \xi} = -\beta N \frac{\partial \theta'}{\partial \xi} \quad \text{at } \xi = 0 \tag{9}$$

The dimensionless parameters are as follows:

1) The parameter $\lambda = k/\sqrt{\alpha t_0} (\epsilon_0 \sigma)^{1/4} (\alpha_{\mathrm{abs}} q_{\mathrm{max}})^{3/4}$ is a measure of the transfer of energy from the incident surface heat flux into the wadi by conduction. With $\epsilon_0 = \alpha_{\mathrm{abs}} = 0.9$ and $q_{\mathrm{max}} = 1300$ W/m^2, the value of λ is 0.04 and 0.66 for native regolith and basalt, respectively.

2) $N = d/\sqrt{\alpha t_0}$ is the ratio of the wadi depth to the thermal penetration depth in it. For a wadi depth of 50 cm of basalt, $N = 0.48$.

3) $N' = (d' - d)/\sqrt{\alpha' t_0}$ is a ratio of the depth of the underlying layer of native regolith to its thermal penetration depth. As mentioned before, while the underlying regolith is of infinite extent, a finite regolith-layer thickness must be chosen for computational purposes. For a layer that is 20 cm thick, $N' = 2.2$.

4) The parameter $\beta = (1/\sqrt{2})(k'/k)\sqrt{\alpha/\alpha'}$ is a measure of the importance of heat loss from the wadi to the underlying regolith layer.

5) $\bar{T}_a = T_a/T_{\mathrm{ref}}$ is the dimensionless environment temperature.

In addition to the previous parameters, the thermal response of the wadi depends on the variation with time of the incident heat flux, the effective surface emissivity, and the heat transferred to the rover. Note that in 1) and 4), the thermal conductivity and diffusivity can be combined and written as $\sqrt{k\rho C_p}$. This quantity appears in many other the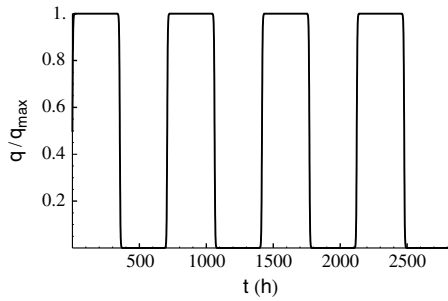rmal applications, such as fire research for the ignition of thermally thick solid fuels [11], where the relationship between ignition delay time and incident radiative heat flux can be used to infer fuel properties ($\sqrt{k\rho C_p}$). Between native regolith and basalt, ρ varies by a factor of less than two, and C_p is about the same. Thus, the thermal conductivity k is the key thermal property that controls the difference in their thermal responses.

B. Incident Solar Flux Profiles

The equatorial solar flux model is shown in Fig. 2. The flux is assumed to be sinusoidal during the daytime and vanishes during the lunar night. The angle between the surface normal and the sun at the peak is further assumed to be the same from lunar month to lunar month. The time period of the solar flux is the synodic period, which is approximately 708 h. The peak heat flux is taken to be $q_{\mathrm{max}} = 1300$ W/m^2. Figure 3 shows how the solar heating of the thermal mass can be enhanced by the use of a reflector that tracks the sun to direct the full solar flux to the surface throughout the lunar day. This constitutes the maximum intensity source of heating without the additional complexity of concentrating or focusing the solar illumination on the surface. The solar flux is a square wave in this case. For numerical purposes, the scaled heat flux is represented as $0.5 + 0.5 \tanh[25 \sin(\pi t/t_0)]$. In reality, the reflector may have some losses, and the flux profile on the wadi surface might be in between what is shown in Figs. 2 and 3.

The solar illumination at the lunar pole is quite different from that at the equator. Figure 4 shows an image of the lunar south pole {2006 Goldstone Solar System Radar (GSSR) background radar back-scatter image [12]}. The large mountain at the top is Malapert, the blue arrow points to the south pole, and the yellow arrow points to a site labeled site A on the rim of Shackleton crater. In this paper, we explore the possibility of constructing a thermal wadi at this particular site. The solar illumination data are based on the 2006 GSSR Jet Propulsion Laboratory digital elevation model (DEM) [12]. It is pixel (14,828, 5711) in the DEM. It is the best-illuminated site near the south pole based on a lowest continuous eclipse time metric.

Figure 5 shows the solar illumination at this site over a compressed time scale. The data start on 1 January 2008 and are in 1 h increments. The illumination is considered to be 100% when the sun angle is larger than the local terrain elevation angle. When the sun angle is smaller than the terrain elevation angle, the sun is blocked, and the illumination is 0%. Partial sun blockages are also possible. The left panel in this figure shows the illumination for about 2.8 years (25,000 h) and includes three polar winters (the dark regions of illumination). The right panel shows the illumination in a portion of the first winter (from 2000 to 3000 h). It is evident that, even during winter, substantial solar illumination is available at this site. In these data, in Fig. 5, the time period with the longest eclipse period (less
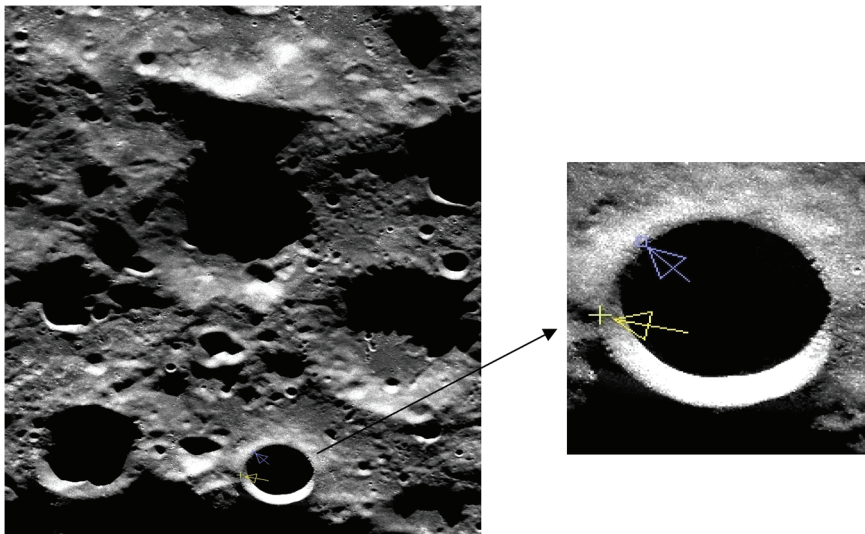

Fig. 3 Equatorial solar flux obtained with the use of a sun-tracking reflector. The solar flux profile is a square wave.

Fig. 4 Site A (yellow arrow) near the lunar south pole (blue arrow) on the rim of Shackleton crater.
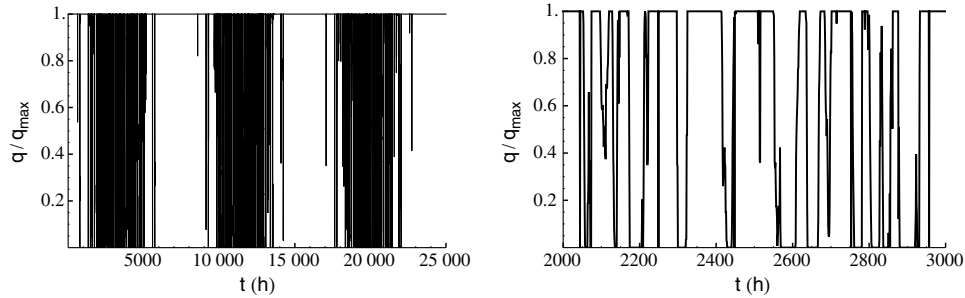
Fig. 5 Solar flux at the polar site with the use of a reflector.

than 100% solar energy) occurs from hour 3256 to 3327 (approximately 71 h). The longest 0% solar flux (approximately 52 h) occurs in the same period. We used the illumination profile shown between $t = 0$ and 6500 h, in Fig. 5, in our thermal model to determine the surface temperature of the wadi. We expect the temperature results in this time period to represent the worst-case scenario at this site.

C. Rover Heat-Loss Considerations

As the principal use of a thermal wadi is to provide a source of sensible heat to a rover during the lunar night, the design of a thermal wadi entails the knowledge of the rate at which energy must be supplied to a rover. Shortly after nightfall, the rover is anticipated to arrive at the location of a thermal wadi to retire for the night. At this time, the rover would be quite warm. A radiation shield is expected to be deployed over the wadi during the night to minimize the heat loss. Therefore, for practically the entire lunar night, the energy exchange between the wadi, the rover, the radiation shield, and free space are all intimately coupled. This is a formidable heat-transfer problem, with time-dependent temperature fields in each of these objects. In this study, we simplify the analysis and represent the rate of energy exchange between the wadi and the rover by a constant nighttime heat flux. To estimate this heat flux, we assume that it is desired to maintain the rover at a given temperature, and the rover is protected by thermal insulation material (such as silica aerogel) of a suitable thickness. There is heat loss by radiation from the exposed surface of the insulation to free space. At steady state, the conduction heat flux through the insulation layer must equal the radiative heat flux from its surface. We choose the rover temperature to be 220 K, which corresponds to the low-temperature tolerance of many electronics components. Assuming a thermal conductivity of 0.01 W/(m · K) for the insulation material, and varying its thickness between 1 and 3 in. and its surface emissivity between 0.2 and 0.8, the rover heat loss is estimated by a one-dimensional heat transfer analysis to be in the range 10 to 25 W/m². In subsequent calculations, we have chosen a constant nighttime surface heat flux of $q_{rov} = 25$ W/m² to represent the rate of energy exchange between the wadi and the rover.

III. Results and Discussion

The results for the temperature in the wadi, chiefly its surface temperature, are presented next, in both lunar equatorial and polar regions. We first show the influence of the various dimensionless parameters on the scaled wadi-surface temperature, in Sec. III.A, for periodic incident solar flux. These results, tabulated in Table 2, are for the scaled (dimensionless) surface temperature. The intent is to show the influence of the various parameters, where a chosen parameter is varied one at a time while the rest are fixed. Sections III.B and III.C discuss selected results for the wadi-surface temperatures near the equator and in the vicinity of the pole, respectively. These results are for the physical surface temperature. This is because, from the points of view of thermal wadi design and operation, it is of interest whether requirements on minimum and maximum temperatures are met and what effects the size and thermal properties of the wadi have on the temperature and amount of energy stored. Since changes in wadi thermal properties affect many of the dimensionless parameters simultaneously, and not just a single parameter, we have chosen to present the wadi-surface-temperature results and their dependence on various design parameters in terms of physical quantities.

The wadi-surface temperatures in both equatorial and polar regions are tabulated in Table 3. It is seen that the maximum wadi temperature is quite insensitive to various wadi design parameters. The theoretical maximum surface temperature is T_{ref}, which was defined earlier, and represents a balance between the absorption of the peak solar flux and the simultaneous radiative emission without heat conduction into the wadi. For $\alpha_{abs} = \epsilon_0 = 0.9$, $T_{ref} = 389$ K when the peak heat flux is 1300 W/m². $T_{ref} = 321$ K, close to the skin-touch temperature of 318 K, when the peak heat flux is reduced to 600 W/m². For a sun angle in the range of 1.5 to 6° near the pole, the peak heat flux is reduced to $1300 \sin(1.5\pi/180) = 34$ W/m² and $1300 \sin(6\pi/180) = 136$ W/m², respectively, and T_{ref} is in the range of 157 to 221 K. With regard to the minimum surface temperature, a limit of 220 K corresponds to the low-temperature tolerance limit of many electronics components. We will refer to this temperature limit to judge the adequacy of various wadi design options. The average surface temperature for equatorial environments is

Table 2 Scaled maximum, minimum, and average wadi-surface temperatures for equatorial solar flux

	N	N'	β	λ	θ_{max} Fourth cycle	θ_{max} Eighth cycle	θ_{min} Fourth cycle	θ_{min} Eighth cycle	θ_{av} Fourth cycle	θ_{av} Eighth cycle
Nominal	0.50	2	0.04	0.65	0.997	0.997	0.668	0.670	0.868	0.869
Varying λ	0.50	2	0.04	0.50	0.998	0.998	0.632	0.634	0.855	0.855
	0.50	2	0.04	0.30	0.999	0.999	0.563	0.564	0.828	0.828
	0.50	2	0.04	0.10	1.000	1.000	0.427	0.428	0.767	0.768
	0.50	2	0.04	0.05	1.000	1.000	0.355	0.356	0.732	0.732
Varying β	0.50	2	0	0.65	0.999	0.999	0.656	0.656	0.866	0.866
	0.50	2	0.02	0.65	0.998	0.998	0.662	0.663	0.867	0.867
	0.50	2	0.06	0.65	0.996	0.996	0.673	0.676	0.869	0.870
	0.50	2	0.08	0.65	0.995	0.996	0.677	0.682	0.869	0.870
Varying N	0.25	2	0.04	0.65	0.998	0.998	0.584	0.586	0.837	0.838
	1.00	2	0.04	0.65	0.998	0.999	0.730	0.735	0.881	0.882
	1.50	2	0.04	0.65	0.993	0.995	0.725	0.741	0.875	0.880
Varying N'	0.50	1	0.04	0.65	0.998	0.998	0.664	0.664	0.868	0.868
	0.50	3	0.04	0.65	0.995	0.996	0.665	0.675	0.866	0.869

obtained by integration of the time-dependent surface temperature during the diurnal cycle. It is not the arithmetic mean of the maximum and minimum surface temperatures. For a wadi of a given size and thermal properties, the average surface temperature is indicative of the amount of energy that is stored in it. Indeed, it can be shown under a periodic steady state (where the net surface heat flux in a cycle vanishes) that the time-averaged temperature at any location is independent of depth within the wadi.

A. Influence of Dimensionless Parameters on the Surface Temperature

The dependence of the maximum, minimum, and average scaled wadi-surface temperatures on the dimensionless parameters N, N', β, and λ is summarized in Table 2. We have assumed that the solar illumination profile is the equatorial profile with a reflector, shown in Fig. 3, $\epsilon_0/\epsilon_1 = 0.3$ and $\bar{q}_{\rm rov} = 0$. For an initial condition, we have used $\theta = \theta' = 0.3$. In Table 2, the range of λ and β covers the thermal property range from native regolith to basalt. N is the dimensionless thermal penetration depth in the wadi, and one would expect its value to be less than one in order to minimize the wadi mass. N' is the dimensionless penetration depth in the underlying regolith layer, and the calculations are expected to be insensitive to it when N' is larger than one. In such cases, however, the calculations must be performed for more diurnal cycles to achieve near-periodic steady-state results. Table 2 includes results for four and eight diurnal cycles that demonstrate that periodic steady-state surface-temperature conditions, as most cases are reached within a few cycles. The maximum wadi temperature is close to one in all cases, and it is quite insensitive to any of the parameters in the ranges shown in Table 2. The values of λ and N have the most effect on the minimum surface temperature, and λ has the most effect on the average surface temperature. Between the four-cycle and eight-cycle results, the minimum surface temperature shows the most change, especially for N and $N' > 1$. Hence, it takes more diurnal cycles to achieve the periodic steady-state minimum temperature for relatively deep layers.

B. Thermal Wadis in Lunar Equatorial Environments
1. Native Regolith with Sinusoidal Heat Flux

As a reference for the various thermal wadi configurations to be explored, the variation with time of the surface temperature of unaltered lunar regolith exposed to the solar flux, described in Fig. 2, was calculated and is shown in Fig. 6. The black curve in Fig. 6 is the result of the present numerical model. The regolith-layer depth is taken to be 20 cm, based on the thermal penetration depth argument given earlier. We assumed that the peak heat flux is 1300 W/m², and the surface absorptivity, daytime emissivity, and nighttime emissivity are equal to 0.9. The overlaid blue curve in Fig. 6 is the periodic steady-state surface temperature that is calculated using Jaeger's method [8], described in the Appendix. It is evident from Fig. 6 that the numerical calculation with a regolith-layer depth of 20 cm is in excellent agreement with the periodic steady-state result for an infinite-depth layer. The maximum and minimum surface temperatures are 387 and 117 K, respectively. With an initial uniform

Fig. 7 Influence of nighttime heat-loss-limiting radiation shield on the thermal wadi-surface temperature vs time for a 50-cm-deep wadi with the thermal properties of basalt rock. $\epsilon_0 = 0.9$ during daytime for all curves (blue curve: $\epsilon_1 = 0.9$; green curve: $\epsilon_1 = 0.5$; red curve: $\epsilon_1 = 0.25$).

temperature of 100 K, conditions close to steady-state oscillations are achieved in four diurnal cycles. For all the equatorial cases, we have used four diurnal cycles in the calculations unless otherwise specified.

2. Basalt Rock with Sinusoidal Heat Flux

The blue curve in Fig. 7 shows the surface-temperature variation with the time of what we describe as a nominal thermal wadi configuration. The nominal equatorial thermal wadi assumes the thermal properties of basalt rock, the thermal conductivity of which is about 100 times that of native regolith, and a wadi depth of 50 cm. The characteristic thermal penetration depth $\sqrt{\alpha t_0}$ in basalt is approximately 100 cm. The surface thermal emissivity is set to a constant, $\epsilon = 0.90$. Compared with that of native regolith, the maximum temperature is reduced slightly from 387 to 375 K, and the minimum temperature increases from 117 to 182 K, but it is not sufficiently warm during much of the lunar night to passively provide heat to a rover or other equipment susceptible to cold. Figure 7 also shows how the surface-temperature variation is altered by the use of the radiation shield that reduces the heat radiated to space from the surface of the thermal mass of the wadi during the lunar night. To simulate the heat-loss-limiting shield, the model adopts an effective surface emissivity reduced from 0.9 during the unshielded daytime configuration to a lower value during the night. The maximum surface temperature is barely affected, while the minimum surface temperature is significantly elevated by the use of a radiation shield ($T_{\rm min} = 233$ K for $\epsilon_1 = 0.25$). The abrupt change in the surface emissivity between daytime and nighttime leads to kinks of small magnitude in the surface-temperature variation. These features are also evident in the results calculated by Jaeger's method [8] for an infinitely deep wadi (see the Appendix).

3. Basalt Rock with Reflector, Radiation Shield, and Rover Heating

Figure 8 shows how the surface temperature of the nominal thermal wadi configuration is changed with the use of a sun-tracking solar illumination reflector (with the solar flux described in Fig. 3) from that shown in Fig. 7 for a sinusoidal flux. From sunrise, it takes
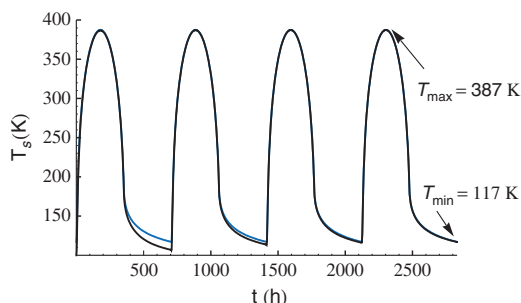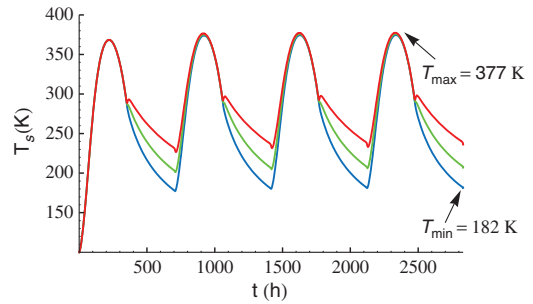

Fig. 6 Surface temperature vs time for native regolith. The equatorial solar flux is as shown in Fig. 2 (black curve: present calculations for a 20-cm-deep layer; blue curve: periodic steady-state result calculated using Jaeger's method [8] for an infinitely deep layer).
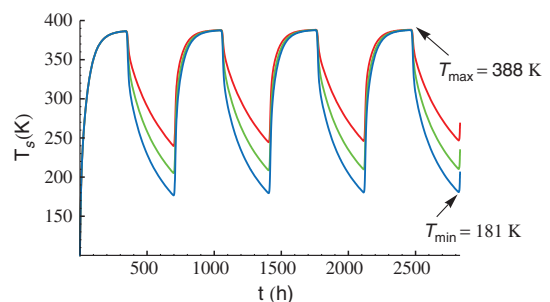

Fig. 8 Surface temperature of an equatorial thermal wadi with a solar reflector, a heat-loss-limiting radiation shield, and rover heating for a 50-cm-deep wadi [$\epsilon_1 = 0.9$ (blue), $\epsilon_1 = 0.5$ (green), and $\epsilon_1 = 0.25$ (red)].

approximately 270 h of absorbing heat for the thermal-mass surface to reach the maximum temperature. The surface remains at this temperature for 80 additional hours, until sunset. Figure 8 includes heat supply to a rover at night and compares the surface temperature of the wadi for various values of the effective nighttime surface emissivity. While the maximum temperature attained is practically the same, variations in the ability of the radiation shield to reduce radiative heat loss greatly affect the minimum temperatures attained during the night, which is in the range 181 K, when the surface is unshielded, to 247 K, when $\epsilon_1 = 0.25$. With the use of the shield, the reflector, and the thermal properties of basalt rock, the thermal mass maintains temperatures high enough to supply heat to a rover or other equipment throughout the equatorial lunar night. From Table 3, the average surface temperature follows the same trend as the minimum

surface temperature. Note that the small kinks in the temperature variation in Fig. 7 just after daylight and nightfall are absent in Fig. 8. The high heat flux provided by the sun-tracking reflector immediately after sunrise and just before the advent of darkness significantly elevates the surface temperature and tends to suppress the influence of abrupt change in the surface emissivity.

4. Influence of Wadi Depth Variation

A key characteristic of the thermal wadi concept is its depth: it affects the mass of material that must be modified to build the wadi and the amount of energy that the wadi can store. Figure 9 shows the results for the wadi-surface temperature, in which the depth of the wadi is varied about the nominal depth of 50 cm, from 25 to 100 cm.

Table 3   Maximum, minimum, and average wadi-surface temperatures in equatorial and near-polar environments

	Wadi depth, m	Regolith-layer depth, m	Wadi thermal diffusivity	Peak heat flux, W/m²	Solar reflector	Radiation shield	ϵ_{night}	Rover heat flux, W/m²	T_{max}, K	T_{min}, K	T_{av}, K
Equatorial	——	0.20	Regolith value	1300	No	No	0.90	0	387	117	232
	——	∞[a]	Regolith value	1300	No	No	0.90	0	387	117	232
	∞[a]	——	Basalt value	1300	No	No	0.90	0	365	215	277
	∞[a]	——	Basalt value	1300	No	Yes	0.50	0	368	237	290
	∞[a]	——	Basalt value	1300	No	Yes	0.25	0	371	257	305
	∞[a]	——	Basalt value	1300	Yes	No	0.90	0	380	230	311
	∞[a]	——	Basalt value	1300	Yes	Yes	0.50	0	382	258	327
	∞[a]	——	Basalt value	1300	Yes	Yes	0.25	0	384	290	344
	0.50	0.20	Basalt value	1300	No	No	0.90	0	375	182	268
	0.50	0.20	Basalt value	1300	No	Yes	0.50	0	376	207	283
	0.50	0.20	Basalt value	1300	No	Yes	0.25	0	377	233	298
	0.50[b]	0.30	Basalt value	1300	No	Yes	0.25	0	378	234	298
	0.50	0.20	Basalt value	1300	Yes	No	0.90	0	388	192	303
	0.50	0.20	Basalt value	1300	Yes	Yes	0.25	0	388	261	339
	0.50	0.20	Basalt value	1300	Yes	Yes	0.25	25	388	247	334
	0.50[b]	0.30	Basalt value	1300	Yes	Yes	0.25	25	388	247	334
	0.25	0.20	Basalt value	1300	Yes	Yes	0.25	25	389	202	318
	1.00[c]	0.20	Basalt value	1300	Yes	Yes	0.25	25	385	279	341
	0.50	0.20	Basalt/5	1300	Yes	Yes	0.25	25	386	236	324
	0.50[c]	0.20	Basalt/10	1300	Yes	Yes	0.25	25	386	219	315
	0.50	0.20	Basalt value	1300	Yes	No	0.90	25	388	181	299
	0.50	0.20	Basalt value	1300	Yes	Yes	0.50	25	388	211	316
	0.50	0.20	Basalt value	1300	Yes	Yes	0.10	25	389	292	354
	0.50 + 1 mm dust[d]	0.20	Basalt value	1300	Yes	Yes	0.25	25	386	255	332
	0.50 + 2 mm dust[d]	0.20	Basalt value	1300	Yes	Yes	0.25	25	381	260	330
	0.50 + 3 mm dust[d]	0.20	Basalt value	1300	Yes	Yes	0.25	25	376	264	327
	0.50 + 4 mm dust[d]	0.20	Basalt value	1300	Yes	Yes	0.25	25	371	267	324
	0.50 + 5 mm dust[d]	0.20	Basalt value	1300	Yes	Yes	0.25	25	365	268	321
	0.50 + 7 mm dust[d]	0.20	Basalt value	1300	Yes	Yes	0.25	25	355	270	315
	0.50 + 10 mm dust[d]	0.20	Basalt value	1300	Yes	Yes	0.25	25	341	269	307
Polar[e]	——	0.20	Regolith value	1300	Yes	Yes	0.25	25	389	171	——
	0.50	0.20	Basalt value	1300	Yes	No	0.90	25	389	261	——
	0.50	0.20	Basalt value	1300	Yes	Yes	0.25	25	389	320	——
	0.50	0.50	Basalt value	1300	Yes	Yes	0.25	25	389	318	——
	0.50	0.75	Basalt value	1300	Yes	Yes	0.25	25	389	319	——
	0.50	0.20	Basalt value	600	Yes	Yes	0.25	25	320	273	——
	0.25	0.20	Basalt value	600	Yes	Yes	0.25	25	321	266	——
	0.10	0.20	Basalt value	600	Yes	Yes	0.25	25	321	241	——
	0.50	0.20	Basalt/5	600	Yes	Yes	0.25	25	321	255	——
	0.50	0.20	Basalt/10	600	Yes	Yes	0.25	25	321	242	——
	0.50	0.20	Basalt value	600	Yes	Yes	0.10	25	321	293	——
	0.50	0.20	Basalt value	600	Yes	Yes	0.50	25	321	251	——
	0.50	0.20	Basalt value	600	Yes	Yes	0.90	25	321	229	——

[a]Jaeger's method .
[b]12th cycle results.
[c]Sixth cycle results.
[d]Fifth cycle results.
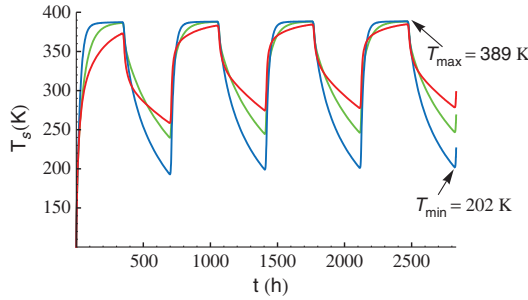[e]Solar illumination profile is as shown in Fig. 5; $0 \leq t \leq 6500$ h.

Fig. 9 **The effect of wadi depth on the surface temperature of an equatorial thermal wadi with a solar reflector, a heat-loss-limiting radiation shield, and rover heating [25 cm (blue), 50 cm (green), and 100 cm (red), each with the thermal properties of basalt].**

The maximum temperature is not very sensitive to the depth of the wadi. The minimum surface temperature is quite sensitive and varies from 202 K, for a depth of 25 cm, to 279 K, for a depth of 100 cm. The corresponding average surface temperatures (from Table 3) are 318 and 341 K. The shallower the wadi, the colder the surface gets, and the average surface temperature is lower. Noting that the average temperature is independent of location within the wadi at steady state, from an energy storage point of view, deeper wadis are preferable, since the mass of the wadi (represented by its depth) and the energy stored per unit mass (represented by the average temperature) are both increased.

5. Influence of Variation of Thermal Diffusivity

The thermal diffusivity of the wadi material also has a significant effect on the minimum surface temperature. A thermal diffusivity that is a factor of 10 smaller than that of basalt (which is about a factor of 10 greater than that of native regolith) results in a minimum surface temperature of about 219 K, as compared with the minimum temperature of 247 K for basalt. Figure 10 shows the wadi-surface temperature when the thermal diffusivity was reduced to as low as one tenth that of basalt.

6. Influence of Dust Covering Wadi Surface

A potential issue of concern is the effect of dust covering the surface of the wadi. It is well known that dust is ubiquitous on the moon. Assuming that the thermal properties of dust (that we regard as fine particles of lunar regolith) are the same as those of native regolith, one can infer that a surface dust layer in excess of 20 cm (of the order of the thermal penetration distance in native regolith) would render the wadi to be completely dysfunctional. Results are reported in Table 3 for the temperature of the wadi surface that is in contact with dust (and not the temperature at the top of the dust layer that is exposed to free space) for dust-layer thickness up to 10 mm. For these calculations, the formalism described earlier has been extended to accommodate regolith layers above and below the wadi. The heat flux balance, given in Eq. (3), is applied at the surface of the dust
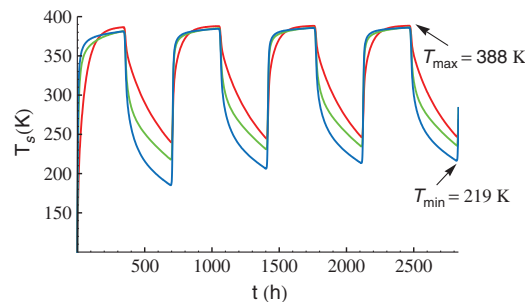
layer. At the interface between the dust layer and the wadi, we assume that temperature and heat flux are continuous. For dust-layer thickness of 5 mm or less, we see that the wadi surface has a smaller temperature swing during the lunar diurnal cycle compared with a situation without any dust. Thus, the dust layer acts to shield the wadi surface from the environment at both temperature extremes. It appears that a dust layer with a thickness of a few millimeter does not degrade the performance of the wadi and might actually help mitigate the temperature swing during the diurnal cycle.

7. Temperature Variation with Distance Beneath Wadi Surface

The temperature variation with distance beneath the surface in a 50-cm-deep wadi with a 30-cm-deep underlying regolith layer is shown in Fig. 11 for constant daytime illumination of the wadi surface. Similar profiles are obtained for sinusoidal daytime illumination as well. The temperature distribution is shown at times close to the extrema of the surface temperature, as well as an intermediate time (see legend in Fig. 11 for the exact times; see Fig. 8 for analogous surface temperatures vs time). In these calculations, the thickness of the underlying regolith layer was increased from 20 to 30 cm to better approximate the unbounded extent of regolith underneath the wadi. Also, 12 diurnal cycles were used, because it takes longer to achieve a periodic steady state for deeper layers, as mentioned earlier. From Table 3, it can be seen that the surface-temperature results for a 50-cm-deep wadi are practically the same with a 20-cm-deep or a 30-cm-deep underlying regolith layer. Figure 11 shows that the influence of the diurnal cycle is not felt significantly beyond approximately 20 cm in the underlying regolith layer. Also, a 50-cm-deep wadi has very little temperature variation with depth, and it can be considered practically isothermal at all times.

C. Thermal Wadis in Lunar Near-Polar Environments

In the vicinity of the lunar poles, the maximum naturally occurring temperature of the lunar soil is far lower than that at lower latitudes because the sun angle is always very oblique (as mentioned before, the theoretical maximum temperature is in the range of 157 to 221 K for a sun angle between 1.5 and 6°). Thus, while the tracking solar reflector could be considered optional in the equatorial sites, it is essential near the poles to heat the wadi adequately. Figure 12 shows the performance of the thermal wadi configuration similar in a near-polar environment similar to the nominal wadi shown by the red curve in Fig. 8. In this calculation, the scaled solar flux variation with time $\bar{q}(t)$, shown in Fig. 5, has been used. The emissivity of the wadi surface is taken to be $\epsilon(t) = (\epsilon_0 - \epsilon_1)\bar{q}(t) + \epsilon_1$, and the heat loss to the rover is defined as $q_{\text{rov}}(t) = C[1 - \bar{q}(t)]$, with $C = 25$ W/m^2. The maximum surface temperature is 389 K, which is the theoretical maximum surface temperature. The minimum surface temperature is about 320 K, and it is obtained at two separate times. This is much higher than the equatorial counterparts because of the extended illumination of the wadi. Figure 13 is a similar plot where the heat-loss-limiting shield has been eliminated. With the surface of the wadi allowed to radiate to space during periods of darkness, the minimum temperature falls to approximately 261 K. The maximum and
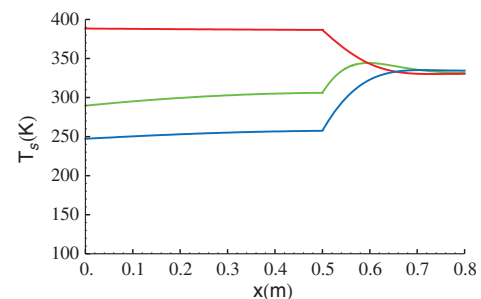

Fig. 10 **The effect of thermal diffusivity on the surface temperature of an equatorial thermal wadi with a solar reflector, a heat-loss-limiting radiation shield, and rover heating for a 50-cm-deep wadi [basalt value (red), one fifth of basalt value (green), and one tenth of basalt value (blue)].**

Fig. 11 **Temperature distribution vs distance below the surface for a 50-cm-deep wadi and a 30-cm-deep underlying regolith layer. The solar flux is as shown in Fig. 3, with 12 diurnal cycles, $q_{\text{rov}} = 25$ W/m^2 [$t = 8127$ h (red), $t = 8307$ h (green), and $t = 8486$ h (blue)].**
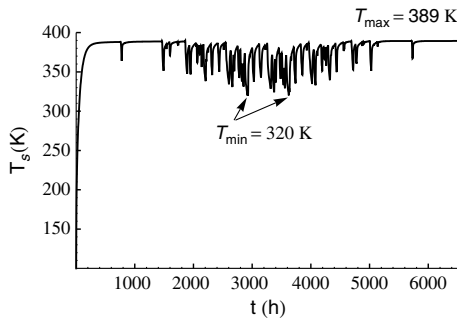
Fig. 12 Surface temperature of the thermal wadi of depth 50 cm, with thermal properties of basalt rock at the lunar polar site using the sun-tracking reflector and the heat-loss-limiting shield. Heat is supplied to a rover during the periods of darkness.

minimum wadi-surface temperatures in the near-polar environment are also summarized in Table 3 for various cases.

Since the summer–winter illumination cycle shown in Fig. 5 has a time period that is an order of magnitude greater than the time period of the diurnal cycle at the equator, the thermal penetration depth (that is proportional to the square root of the time period) is approximately three times as large at the pole than at the equator. We therefore studied the influence of the thickness of the underlying regolith layer (0.2, 0.5, and 0.75 m; see Table 3) on the surface temperature of the wadi. The maximum deviation in the wadi-surface temperature between the 0.2 and 0.75 m regolith-layer thicknesses is 1.6 K, and the maximum deviation between the 0.5 and 0.75 m regolith-layer thicknesses is 0.3 K. We have used results for the wadi-surface temperature with 0.2 m as the regolith-layer thickness in Figs. 12 and 13. We also checked the sensitivity of the minimum temperature in Fig. 13 by using the initial condition $T = 100$ K at $t = 1000$ h (instead of $t = 0$ h) and the initial condition $T = 300$ K (instead of $T = 100$ K) at $t = 0$ hr. In both cases, the change in the minimum temperature is less than 0.5 K.

It might be safer for suited astronauts and equipment to reduce the maximum temperature to be close to the skin-touch temperature limit of 318 K. Table 3 shows that when the peak heat flux is reduced to 600 W/m^2 while keeping the loss-limiting shield during periods of darkness, the maximum and minimum surface temperatures achieved are 320 and 273 K, respectively. We also note that for the equatorial case, if the radiation shield is used approximately 100 h before sunset, then the wadi-surface temperature at sunset will be lower than the touch temperature of 318 K. This strategy is difficult to simulate in the polar case, since the duration of lighted periods and the onset of darkness are irregular.

The effect of building the wadi to a shallower depth in the lunar polar environment and relaxing the thermal diffusivity to fractional values of the diffusivity of basalt rock are also presented in Table 3. Reducing the wadi depth reduces the minimum surface temperature. For a wadi depth of 10 cm, the minimum surface temperature is about 241 K. When the wadi thermal diffusivity is reduced by a factor of 10 from the basalt value, the minimum surface temperature is about 242 K. These temperatures are above the tolerance limit of 220 K for electronic equipment.
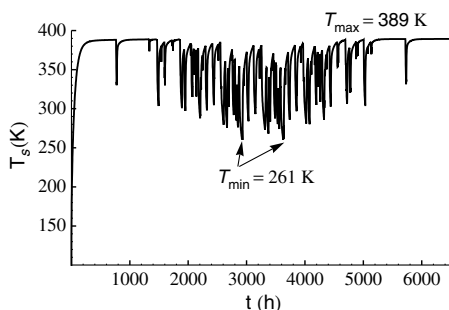

Fig. 13 Same as Fig. 12 but without the heat-loss-limiting shield.

IV. Conclusions

The objective of this study was to determine the answer to the question: can engineered thermal wadis function as safe havens for exploration assets, protecting them from the extreme cold of lunar darkness? The present analysis provides an affirmative answer to this question. That is, the analysis shows that thermal wadis of the present concept, if constructed on the lunar surface using modified regolith as the thermal mass, can protect exploration assets from the extremely cold conditions that are otherwise encountered on the lunar surface. A significant advantage of the concept is the use of modified lunar regolith as the thermal-mass material, thereby substantially reducing the mass that must be brought from Earth to manufacture it.

Other than in a permanently shadowed crater at either of the lunar poles, the two cases considered represent reasonable bounds of the best case (Shackleton crater rim, with a maximum period of darkness of about 52 h) and the worst case (equatorial locations with maximum periods of darkness of about two Earth weeks). In either case, if the thermal mass has a reasonable depth, if energy is stored in the thermal mass in sufficient quantities through the use of a reflecting surface, if heat loss by radiation is controlled through the use of a radiant energy reflector, and if suitable thermophysical properties are achieved when producing the thermal mass, the analysis shows that thermal-mass temperatures can be maintained typically greater than 230 K. Engineering tradeoffs can be made with respect to the design of the thermal wadi and the design of the system that must be placed on the moon in order to produce thermal-mass materials and assemble the thermal wadi so as to meet specific temperature requirements and optimize the mass of what must be launched from Earth while also taking into account other requirements related to reliability and performance.

We can also contemplate improvements to the design of the thermal wadi that provide a greater amount of energy storage. For example, solar concentrators can be provided that focus more energy flux and charge the thermal mass with more energy than we have considered in our analyses, and the radiant energy reflector can be designed to be more efficient, yielding lower effective emissivities and further reducing heat loss. Likewise, if a small amount of encapsulated phase change material (e.g., paraffin wax) is brought from Earth and incorporated in the thermal mass, greater energy storage capacity will be enabled coincident with reduced temperature ranges. While these features have not been considered in our thermal analysis, it is nevertheless clear that they would provide improvements to the functionality of the thermal wadi.

Appendix: Periodic Steady State

When the solar flux is periodic, we expect the surface temperature of the wadi to eventually achieve a periodic steady state. As mentioned earlier, Jaeger [8] has developed a model to calculate the periodic steady-state temperature of the surface of the moon. While Jaeger assumed that the bulk thermal properties of regolith and the surface radiative properties are constant in space and time in the calculations that he reported, his model is actually more general and can account for variations in the surface radiative properties during the diurnal cycle. Therefore, we are able to capture the influence of a radiation shield used during the lunar night by employing his model. An extension of the model, to account for thermal properties that are varying in space (such as in a wadi of a finite depth with an infinite amount of regolith below it), does not appear to be available in the literature. We therefore assume that the medium is infinitely deep with constant properties. The periodic steady state, with time period $2t_0$, is divided into J uniform intervals $j = 1, J$. The fundamental result derived by Jaeger is that if the surface temperature of the medium is maintained at unity in the first interval $j = 1$ and zero in the remaining intervals $j = 2, J$ in every period, then at steady state, the average heat flux into the medium in the jth interval is $\sqrt{(k\rho C_p/2\pi t_0)}\phi_j$, where

$$\phi_1 = 2\sqrt{J} - \frac{2J}{\sqrt{\pi}} \int_0^\infty \frac{(1 - e^{-z^2/J})[e^{-(J-1)z^2/J} - e^{-z^2}]}{z^2(1 - e^{-z^2})} \, dz \quad \text{(A1)}$$
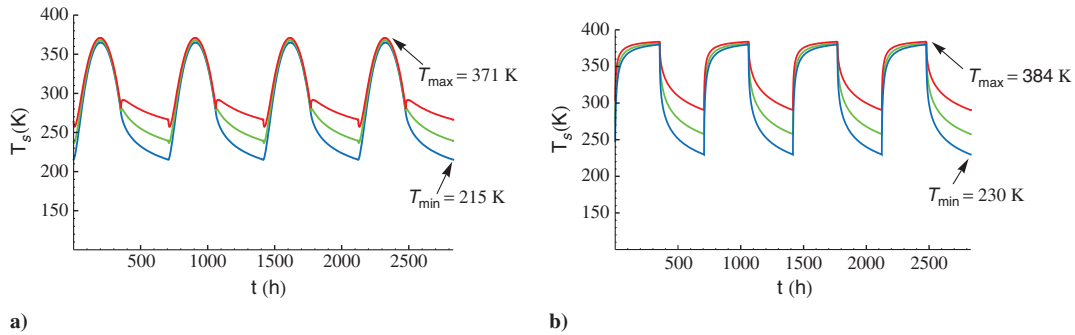
Fig. A1 Periodic steady-state surface temperature calculated employing Jaeger's method [8] for an infinitely deep basalt layer for a) sinusoidal heat flux and b) a square wave heat flux. Peak flux = 1300 W/m². $\epsilon_0 = 0.9$ during daytime for all curves (blue curve: $\epsilon_1 = 0.9$; green curve: $\epsilon_1 = 0.5$; red curve: $\epsilon_1 = 0.25$).

and for $j = 2, J$,

$$\phi_j = 2\sqrt{J}(\sqrt{j} + \sqrt{j-2} - 2\sqrt{j-1})$$
$$- \frac{2J}{\sqrt{\pi}} \int_0^\infty \frac{e^{-(j-1)z^2/J}(1 - e^{-z^2/J})[e^{-(J-1)z^2/J} - e^{-z^2}]}{z^2(1 - e^{-z^2})} \, dz \quad (A2)$$

If the surface temperature has values $T_{s_1}, T_{s_2}, \dots, T_{s_J}$ for $j = 1, J$, then the heat flux into the medium in the jth interval is

$$f_j = \sqrt{\frac{k\rho C_p}{2\pi t_0}} \sum_{i=1}^{J} T_{s_i} \phi_{j-i+1} \quad (A3)$$

(Note that, in this expression, $\phi_0, \phi_{-1}, \cdots$ are equal to $\phi_J, \phi_{J-1}, \cdots$).

Assuming that the incident solar flux is as shown in Fig. 2, the surface heat flux can be written during the day and night, respectively, as

$$f(t) = \alpha_{abs} q_{max} \sin(\pi t/t_0) - \epsilon\sigma(T_s^4 - T_a^4) \quad \text{for } 0 \leq t \leq t_0 \quad (A4)$$

$$f(t) = -\epsilon\sigma(T_s^4 - T_a^4) \quad \text{for } t_0 \leq t \leq 2t_0 \quad (A5)$$

We have used $\epsilon = \epsilon_0$ in Eq. (A4) and $\epsilon = \epsilon_1$ in Eq. (A5) to determine the influence of a radiation shield used during the night. Once ϕ_j is determined for each j, Eqs. (A3–A5) yield a set of nonlinear algebraic equations for the unknown temperatures $T_{s_1}, T_{s_2}, \dots, T_{s_J}$ for $j = 1, J$. We used Newton's method to solve the nonlinear system of equations, with $J = 1501$ (Jaeger used $J = 21$ [8]).

The periodic steady-state results for native regolith with a sinusoidal heat flux are shown in Fig. 6. Similar results for an infinitely deep basalt layer in the presence of a nighttime radiation shield are shown in Figs. A1a and A1b for a sinusoidal and a square wave heat flux, respectively. Results for a finite basalt layer after four diurnal cycles are shown earlier in Fig. 7. Comparing Figs. 7 and A1a, we see that the maximum surface temperature is elevated, and the minimum surface temperature is reduced for a wadi of a finite depth compared with those for an infinitely deep wadi. Note that the abrupt change in emissivity between day and night leads to kinks of small magnitude in the surface temperature that are evident in both Figs. 7 and A1a. These are suppressed for the square wave heat flux results in Fig. A1b, as well as for a finite-depth basalt wadi in Fig. 8.

Acknowledgments

References

[1] Wegeng, R. S., Mankins, J. C., Balasubramaniam, R., Sacksteder, K., Gokoglu, S. A., Sanders, G. B., and Taylor, L. A., "Thermal Wadis in Support of Lunar Science and Exploration," 6th International Energy Conversion Engineering Conference, AIAA Paper 2008-5632, July 2008.

[2] Balasubramaniam, R., Wegeng, R. S., Gokoglu, S., Suzuki, N., and Sacksteder, K., "Analysis of Solar-Heated Thermal Wadis to Support Extended-Duration Lunar Explorations," 47th AIAA Aerospace Sciences Meeting and Exhibit, AIAA Paper 2009-1339, Jan. 2009.

[3] Colozza, A. J., "Analysis of Lunar Regolith Thermal Energy Storage," NASA CR 189073, 1991.

[4] Heiken, G. H., Vaniman, D. T., and French, B. M. (eds.), *The Lunar Sourcebook: A User's Guide to the Moon*, Cambridge Univ. Press, New York, 1993.

[5] Taylor, L. A., and Meeks, T. T., "Microwave Sintering of Lunar Soil: Properties, Theory, and Practice," *Journal of Aerospace Engineering*, Vol. 18, No. 3, 2005, pp. 188–196.
doi:10.1061/(ASCE)0893-1321(2005)18:3(188)

[6] Taylor, L. A., and Carrier, W. D., III, "Oxygen Production on the Moon: An Overview and Evaluation," *Resources of Near-Earth Space*, Univ. Of Arizona, Tucson, AZ, 1993, pp. 69–108.

[7] Wesselink, A. J., "Heat Conductivity and the Nature of the Lunar Surface Material," *Bulletin of the Astronomical Institutes of The Netherlands* Vol. 10, 1948, pp. 351–363.

[8] Jaeger, J. C., "Conduction of Heat in a Solid with Periodic Boundary Conditions, with an Application to the Surface Temperature of the Moon," *Proceedings of the Cambridge Philosophical Society (Mathematical and Physical Sciences)*, Vol. 49, No. 2, 1953, pp. 355–359.
doi:10.1017/S0305004100028450

[9] Mitchell, D. L., and de Pater, I., "Microwave Imaging of Mercury's Thermal Emission at Wavelengths from 0.3 to 20.5 cm," *Icarus*, Vol. 110, No. 1, 1994, pp. 2–32.
doi:10.1006/icar.1994.1105

[10] Vasavada, A. R., Paige, D. A., and Wood, S. E., "Near-Surface Temperatures on Mercury and the Moon and the Stability of Polar Ice Deposits," *Icarus*, Vol. 141, No. 2, 1999, pp. 179–193.
doi:10.1006/icar.1999.6175

[11] Tewarson, A., "Generation of Heat and Chemical Compounds in Fires," *The SFPE Handbook of Fire Protection Engineering*, 3rd ed., National Fire Protection Assoc., Quincy, MA, 2002, pp. 3–161.

[12] Fincannon, H. J., "Lunar Polar Illumination for Power Analysis," 6th International Energy Conversion Engineering Conference, AIAA Paper 2008-5631, July 2008.